

1 **GEE-PICX: Generating cloud-free Sentinel-2 and**
2 **Landsat image composites and spectral indices**
3 **for custom areas and time frames - a Google**
4 **Earth Engine web application**

5

6 **LUISA PFLUMM^{1,2}, HYEONMIN KANG^{1,2,3}, ANDREAS WILTING¹, JÜRGEN NIEDBALLA^{1*}**

7

8 *¹ Leibniz Institute for Zoo and Wildlife Research, Alfred-Kowalke-Str. 17, 10315 Berlin, Germany*

9 *² University Würzburg, Sanderring 2, 97070 Würzburg*

10 *³ Nadar GmbH, Kasseler Str. 42, 04155 Leipzig, Germany*

11

12 * Corresponding author: niedballa@izw-berlin.de

13

14

15

16

17

This manuscript is a non-peer-reviewed preprint submitted to EarthArXiv.

18 Abstract

- 19 1. Earth observation satellites are collecting vast amounts of data that are both free and
20 openly accessible. These data have immense potential to support environmental,
21 economic, and social fields. However, along with the increasing availability of remotely
22 sensed data, challenges are also increasing in accessing and processing these data. In
23 particular, easy-to-use solutions for accessing and computing cloud-free image
24 composites from often cloudy satellite data are lacking, preventing researchers and
25 practitioners without in-depth training in remote-sensing techniques to use the accessible
26 satellite data.
- 27 2. We developed GEE-PICX, a web application with an intuitive user interface in the cloud
28 computing platform Google Earth Engine to overcome these challenges and to create
29 cloud-free and analysis-ready image composites for user-defined areas and time steps
30 based on Sentinel-2 and Landsat 5, 7, 8, and 9 images. Data coverage is global and image
31 composites can be aggregated annually or seasonally. The earliest available data are
32 from 1984 (launch of Landsat 5).
- 33 3. The workflow automatically filters all available satellite data according to user input and
34 removes clouds, cloud shadows, and snow. It returns spectral band information, calculates
35 a variety of spectral indices and returns the number of valid scenes per pixel as a quality
36 assessment band.
- 37 4. GEE-PICX provides researchers with no or little experience in remote sensing for the first
38 time a customizable tool for creating custom data products from freely accessible satellite
39 data with extensive temporal and global spatial coverage. Server-side data processing
40 ensures the tool is usable without hardware limitations. The simple export of time series
41 of ready-to-use rasters including numerous spectral indices can greatly assist
42 environmental programmes and biodiversity research in a variety of disciplines.

43 Introduction

44 Understanding environmental changes such as deforestation, desertification, urbanization, or the
45 expansion of croplands over time is of utmost importance to quantify the anthropogenic impacts
46 on earth and to support sustainable development and environmental protection (Chaves et al.,
47 2020; Mallinis & Georgiadis, 2019; Weng et al., 2008). Satellite remote sensing is a widely used
48 method for monitoring such environmental changes due to the multitude of available sensors and
49 platforms providing continuous data of the earth's surface (Cord et al., 2017). Remote sensing
50 data is often freely available (e.g. Landsat since the 1980s), enabling scientists to monitor and
51 quantify short- and long term environmental changes. Optical remote sensing imagery provides
52 (multi-)spectral information, yet the presence of clouds, cloud shadows, and highly reflective
53 surfaces such as snow can adversely affect sensor measurements, posing challenges in
54 acquiring unbiased and gap-free information (Zhu et al., 2015). Opaque clouds cover
55 approximately 31% of the Earth's surface at any time (Guzman et al., 2017), necessitating
56 automatic detection and accurate removal from remote sensing data prior to analysis to prevent
57 data errors at the respective positions. Cloud removal causes gaps in satellite images which can
58 complicate analysis. This can be overcome by merging multiple images from different time points
59 to create cloud-free and gap-free image products. These products can then be used for land cover
60 classifications (Verhoeven & Dedoussi, 2022), land monitoring applications (Carrasco et al., 2019;
61 Parmes et al., 2017), time series analyses (Lasaponara et al., 2022; Yin et al., 2020) or spatial
62 modeling (Guharajan et al., 2021).

63 After cloud-correction, multi-spectral information can either be used directly (Zhu et al., 2018) or
64 via derived spectral indices, which are combinations of the spectral reflectance from two or more
65 wavelengths (Chaves et al., 2020; Rudd et al. 2021). Spectral indices are often more suitable for
66 specific analyses than the raw spectral information due to more clearly defined and interpretable

67 properties (Rudd et al., 2021). The most popular spectral indices are vegetation indices, but other
68 indices for burned areas, man-made (built-up) features, or water are available, too (Chaves et al.,
69 2020; Petropulos & Kalaitzidis, 2011).

70 Generating analysis-ready remote sensing data and derived products (e.g. spectral indices) is,
71 however, often challenging, particularly for long-term analyses over larger regions. Creating
72 cloud-free mosaics is often only possible for well-trained remote-sensing scientists. Besides
73 technical expertise, it requires considerable computational resources to process hundreds or
74 thousands of remote sensing data sets. Here, cloud computing platforms such as Google Earth
75 Engine (GEE), powered by the Google Cloud infrastructure, offer new possibilities for big data
76 analysis (Lasaponara et al., 2022; Piao et al., 2019; Yang et al., 2021).

77 To overcome these challenges, we developed GEE-PICX, a Google Earth Engine web application
78 for generating and exporting cloud-free and analysis-ready composites of satellite images for
79 user-defined areas and time steps with global data coverage. We followed four design principles
80 in developing GEE-PICX:

- 81 **1. Flexibility of user input.** Users have control over choice of satellite platform (Landsat or
82 Sentinel-2), study area boundaries, time range, maximum cloud cover (for single images),
83 aggregation mode, and image bands. Relevant images are automatically selected from
84 the data catalog according to user input.
- 85 **2. Ease of use.** The application features a self-explanatory interface, requires only a Google
86 account, a web browser and internet connection, and has no hardware or software
87 requirements thanks to server-side processing.
- 88 **3. Export of large data sets.** Only limited by Google drive storage capacity.

89 **4. Generate analysis-ready data.** Generates cloud-free image mosaics with spectral
90 bands, spectral indices, and a quality assessment band (valid scenes per pixel). Export
91 image resolution and coordinate reference system are customizable.

92 The application allows users without experience in remote sensing to generate cloud-free and
93 analysis-ready image composites for custom study areas and points in time for a multitude of
94 applications in ecology and beyond. Compared to other platforms that allow downloading similar,
95 analysis-ready products it also provides information on data quality or spectral indices which is
96 not provided by EarthExplorer (United States Geological Survey, 2023) and it allows significantly
97 larger downloads than SentinelHub (Sinergise, 2023a).

98 Workflow description

99 Overview

100 Users can access the web application via the provided application link (see Data availability). The
101 script is written in JavaScript and commented to facilitate orientation. No manual code
102 adjustments are necessary. With the application running, users can define parameters according
103 to their requirements in the application interface next to the map. The application then internally
104 processes user inputs, executing functions for satellite image (pre-)processing, visualization, and
105 export preparation. Data visualizations are available directly in the application. The products can
106 be exported at user-defined spatial resolutions and coordinate systems and are ready to use for
107 subsequent analyses.

108 User input

109 Below we provide a detailed overview of the choices users can make for creating customized data
110 exports. For advanced information on data processing see [Supporting Information S1](#).

111 **Satellite data:** The application can provide image composites based on either the Landsat or the
112 Sentinel-2 mission. Both Landsat and Sentinel-2 datasets consist of atmospherically and
113 topographically corrected Level-2A products that show surface reflectance values with
114 atmospheric correction applied. The dataset choice can be based on either the required spatial
115 resolution or length of the time series. The earliest Level-2A products from Landsat date back to
116 1984 (at 30m resolution), whereas Sentinel-2 Level-2A products have been available since 2017
117 (at 10m resolution). The availability of Landsat data from the late 1980s and early 1990s is much
118 lower than in recent years, when more Landsat missions are simultaneously acquiring imagery at
119 a higher temporal frequency. When selecting Landsat as the platform, users have the option to
120 include imagery from all Landsat missions (5-9) to create image composites, or they can choose
121 to include only Landsat-8 and 9 data. The second option is useful to avoid including erroneous
122 Landsat-7 images affected by the Scan Line Corrector failure in 2003 (United States Geological
123 Survey, 2022). However, Landsat-8 data are only available from 2013 and Landsat-9 data from
124 2022. For more specific information on the satellite missions see [Supporting Information S2](#).

125 **Area of interest:** The boundary of the study area can be defined either by uploading a shapefile
126 as an Earth Engine asset (Google Earth Engine, 2021), or by manually drawing a polygon on the
127 Google Earth Engine map. Data coverage is global.

128 **Time period:** The time frame can be specified by year- and month range. By default, scenes are
129 aggregated for one year (months 1 - 12). Users can create seasonal image aggregates by
130 narrowing the selection to specific consecutive months (also crossing the year boundary). Users
131 can request export of imagery from multiple years at once.

132 **Cloud cover filter:** Optical satellite images may exhibit partial or complete cloud coverage. The
133 pixel-level cloud masks included in scenes cannot perfectly detect and filter out all clouds and
134 cloud shadows (Sanchez et al., 2020). Therefore, the cloud cover percentage per scene is utilized
135 to enhance the quality of image composites by removing scenes exceeding a cloud cover
136 threshold. By default, images with cloud cover exceeding 65% are excluded prior to aggregation.
137 Opting for a 100% threshold includes all images captured within the specified study area and time
138 frame.

139 **Image bands:** Users can select single or multiple spectral bands, as well as spectral indices and
140 a valid pixel band, by activating the corresponding checkboxes. Spectral bands convey surface
141 reflectance data and are correlated with chlorophyll and other pigments, vegetation structure and
142 water content (Petropulos & Kalaitzidis, 2012). Key correlations include Green, Red, and Red-
143 edge bands with chlorophyll and pigments, NIR bands with leaf structure, and SWIR with
144 vegetation structure and water content (Chaves et al., 2020; Fernández-Manso et al., 2016).
145 Spectral indices result from mathematical combinations of the spectral bands (see [Supporting](#)
146 [Information S3](#) for details on all available indices). The valid pixel band is a quality assessment
147 layer specifying the number of valid scene values that are aggregated at each pixel.

148 **Aggregation mode:** The aggregation mode determines which summary statistic is applied to the
149 pixel values of all selected images. Available choices are mean, median and standard deviation.

150 **Coordinate system:** The application offers the choice to export rasters in UTM and WGS 84
151 (EPSG 4326) formats. If UTM is selected, the application automatically identifies the appropriate
152 zone. If the study area spans multiple UTM zones, images can only be exported in WGS 84.

153 **Spatial pixel resolution:** The application provides the options to export images at four different
154 spatial resolutions ranging from 10 to 100 meters. Opting for high resolutions in extensive study
155 areas could yield products exceeding several gigabytes, potentially posing challenges for

156 subsequent analyses. Users should choose a resolution that matches their research or monitoring
157 objectives.

158 Image export

159 After initiating the export in the application user interface, users can inspect and execute the
160 actual image export(s) within the upper-right window via the Console and Tasks tabs (see Data
161 availability). Two image collections will be automatically added to the Console. The first contains
162 all individual satellite images after filtering, the second contains the image aggregates available
163 for export. Each annual / seasonal image that appears in the *Tasks* manager needs to be exported
164 individually. When clicking "Run", a pop-up window will appear in which the user can optionally
165 modify export names, coordinate reference system, scale, export destination and file format.

166 The easiest way to save the files on a local computer is to export them to a Google drive folder
167 which is connected to the users' Google account, and then download the data from there. Multiple
168 image exports run in parallel and depending on study area size each export can take from minutes
169 to hours (or even days for study regions measuring hundreds of thousands of square kilometers).
170 When exporting large datasets, Google Earth Engine splits each image into smaller tiles. After
171 downloading them from Google Drive, they can either be merged to a large contiguous mosaic,
172 or be used as a virtual raster.

173 Except for the "valid-pixel" band, all band values of the export images are multiplied by 10,000.
174 This allows the raster values to be stored as integer values (signed 16-bit) instead of floating point
175 values, thus reducing the file size of exports.

176 Data visualization

177 Users can visualize their export data on the map by selecting either a spectral index or various
178 band combinations. Band combinations can highlight certain features (e.g., vegetation types,
179 water bodies, and urban areas) due to correlations between measurable biophysical properties
180 on the Earth's surface and remotely sensed surface reflectance (Price et al., 2002). After choosing
181 the visualization parameter, all aggregated images will be added to the map with default
182 visualization settings. Adjustments to visualization parameters can be made individually within the
183 map's layer panel box (follow instructions on Github link, see Data availability). All indices have a
184 valid value range from -1 to 1 in the application, while the band values of export images are
185 multiplied by 10,000 (except for the valid pixel band). Google Earth Engine may encounter
186 computational problems for visualization if the data is too large due to the size of the study area
187 and/or the length of the time period. This may lead to scaling error messages and some objects
188 would not be displayed on the map (or also *Console*). Visualization problems, however, do not
189 affect image exports, which are always possible and only limited by the storage capacity of the
190 user's Google drive.

191 In addition to the visualization options in Google Earth Engine, we provide an interactive R Shiny
192 application for visualizing image time series (see Data Availability).

193 Case examples

194 Example A shows deforestation in Brasil using historical Landsat images, while Example B
195 focusses on seasonal land cover changes in the city of Würzburg (Germany), emphasizing the
196 enhanced level of detail provided by Sentinel-2 imagery ([Figure 1](#)). In both examples a
197 combination of three spectral bands (SWIR1-NIR-R; NIR-R-G) and a spectral index (NDVI) are

198 shown together with the number of valid pixels (see Fig. 1). The data contain more spectral bands
199 and indices not shown here.

200 In the Amazon rainforest, deforestation has become a pressing environmental concern over the
201 past several decades. Soy farms, along with other agricultural expansion, have played a
202 significant role in driving deforestation in the Amazon (Nepstad et al., 2006). We used GEE-PICX,
203 to generate and export annual image aggregates for an area in Ariquemes, Rondônia, Brasil for
204 1991 and 2021, illustrating the magnitude of change over three decades. Such annual aggregates
205 (or composites) are suitable for inferences on broad trends, but average seasonal dynamics or
206 land cover changes within a year, making them unsuitable e.g. for mapping floods.

207 The second example shows the seasonal changes in land cover/land use in the city center of
208 Würzburg, Germany, and highlights the surrounding ring-shaped park. The region's transition
209 between summer and winter was captured in seasonal satellite image composites and showcases
210 the distinct phenological variations. The higher spatial resolution of Sentinel-2 imagery allows
211 better discrimination of small-scale features and proves particularly valuable in the context of land
212 cover and land use monitoring. Seasonal variation in cloud cover can lead to seasonal bias in the
213 available data. Snow cover can also affect the quality of seasonal image compositions because
214 the applied cloud mask algorithm (see [Supporting Information S1](#)) does not perfectly mask highly
215 reflective surfaces such as clouds or snow in individual scenes. Cloud masking leads to data gaps
216 in all affected images. If all scenes have data gaps at the same pixels, the image composite will
217 also have data gaps at this location. During the export to Google drive Google Earth Engine
218 assigns a value of zero to data gaps in image composites, potentially biasing subsequent
219 analyses. Zero values at these locations should be converted to NA prior to further analyses (see
220 Data availability).

221 Conclusion

222 The use of satellite imagery is essential for many environmental and conservation studies.
223 However, the broad use of freely available satellite products currently requires expertise in data
224 selection and pre-processing, as well as computational resources. Many environmental and
225 conservation studies therefore primarily rely on pre-packaged thematic products (Wong et al.,
226 2022). However, these datasets often lack the necessary detail to address specific research
227 questions, despite the wealth of information present in satellite data. GEE-PICX provides a
228 solution for users across various domains by significantly simplifying access to the creation of
229 cloud-free satellite image composites. It effectively addresses problems of cloud cover, which are
230 particularly challenging in tropical or mountainous regions (Sanchez et al., 2020; Hribljan et al.,
231 2017). Through the intuitive and user-friendly GEE-PICX application, users can easily generate
232 and export (multi-)temporal cloud-free satellite images for any region and any time period starting
233 from 1984 (availability varies by region).

234 The multispectral information in the generated products are complemented by additional
235 information on spectral indices and data quality. These are typically not present in the generated
236 output of other platforms. GEE-PICX is further set apart by allowing data generation of extensive
237 areas with very large download sizes. By making the freely available archives of Landsat and
238 Sentinel-2 accessible for non-remote-sensing scientists and practitioners, GEE-PICX strongly
239 supports integrating these archives in environmental and conservation projects of various fields.

240

241 Acknowledgements

242 We would like to express our gratitude to several individuals and organizations who have played
243 an important role in the successful completion of this project. First of all, we would like to thank
244 Marius Philipp, who gave us great technical support as a tutor during workflow and app
245 development in Google Earth Engine. Moreover, we thank Matthias Baumann and Julian Oeser
246 for insightful discussions about processing and utilization of satellite data time series. The work
247 was financially supported by the Leibniz Institute for Zoo and Wildlife Research and parts of the
248 work were done during the implementation of the USAID funded Biodiversity Conservation project
249 in Viet Nam (7204402CA00001).

250 Conflict of Interest statement

251 The authors declare no conflicts of interest.

252 Author contributions

253 Jürgen Niedballa and Andreas Wilting conceived the idea, Luisa Pflumm led the development of
254 the GEE script and Hyeonmin Kang led the development of the GEE App user interface. Luisa
255 Pflumm developed the case examples. Luisa Pflumm, Jürgen Niedballa and Andreas Wilting led
256 the writing of the manuscript, and Hyeonmin Kang contributed to the drafts. All authors gave final
257 approval for publication.

258 Data availability

259 The link to the GEE-PICX application is provided on this Github page: [https://github.com/Luisa-](https://github.com/Luisadel/GEE-PICX)
260 [del/GEE-PICX](https://github.com/Luisadel/GEE-PICX). The GitHub page also contains a detailed user guide.

261 In order to use the GEE-PICX application, users need to log in to Google Earth Engine using their
262 Google account. The application opens in JavaScript code editor mode to allow for data export.
263 From the application, user inputs are specified and products can be exported to users' Google
264 drive for download.

265 An R script to convert null values of an exported raster to NA is provided on Github. We
266 furthermore provide an R Shiny app to visualize and query time series of annual images
267 downloaded via GEE-PICX on GitHub.

268 References

269 Carrasco, L., O'Neil, A. W., Morton, R. D., & Rowland, C. S. (2019). Evaluating combinations of
270 temporally aggregated Sentinel-1, Sentinel-2 and Landsat 8 for land cover mapping with Google
271 Earth Engine. *Remote Sensing*, 11(3), 288.

272 Chaves, E.D.M., Picoli, C.A.M., & Sanches, D.I. (2020). Recent applications of Landsat 8/OLI and
273 Sentinel-2/MSI for land use and land cover mapping: A systematic review. *Remote Sensing*,
274 12(18), 3062.

275 Cord, A. F., Brauman, K. A., Chaplin-Kramer, R., Huth, A., Ziv, G., & Seppelt, R. (2017). Priorities
276 to advance monitoring of ecosystem services using earth observation. *Trends in ecology &*
277 *evolution*, 32(6), 416-428.

278 Google Earth Engine (2021). Managing assets. [https://developers.google.com/earth-](https://developers.google.com/earth-engine/guides/asset_manager)
279 [engine/guides/asset_manager](https://developers.google.com/earth-engine/guides/asset_manager) (accessed on 11 July 2023).

280 Guharajan, R., Mohamed, A., Wong, S. T., Niedballa, J., Petrus, A., Jubili, J., ... & Wilting, A.
281 (2021). Sustainable forest management is vital for the persistence of sun bear *Helarctos*
282 *malayanus* populations in Sabah, Malaysian Borneo. *Forest Ecology and Management*, *493*,
283 119270.

284 Guzman, R., Chepfer, H., Noel, V., Vaillant de Guélis, T., Kay, J. E., Raberanto, P., ... & Winker,
285 D. M. (2017). Direct atmosphere opacity observations from CALIPSO provide new constraints on
286 cloud-radiation interactions. *Journal of Geophysical Research: Atmospheres*, *122*(2), 1066-1085.

287 Hribljan, J. A., Suarez, E., Bourgeau- Chavez, L., Endres, S., Lilleskov, E. A., Chimbolema, S.,
288 ... & Chimner, R. A. (2017). Multidate, multisensor remote sensing reveals high density of
289 carbon- rich mountain peatlands in the páramo of Ecuador. *Global change biology*, *23*(12), 5412-
290 5425.

291 Lasaponara, R., Abate, N., Fattore, C., Aromando, A., Cardettini, G., & Di Fonzo, M. (2022). On
292 the Use of Sentinel-2 NDVI Time Series and Google Earth Engine to Detect Land-Use/Land-
293 Cover Changes in Fire-Affected Areas. *Remote Sensing*, *14*(19), 4723.

294 Mallinis, G., & Georgiadis, C. (2019). Editorial of Special Issue "Remote Sensing for Land
295 Cover/Land Use Mapping at Local and Regional Scales". *Remote Sensing*, *11*(19), 2202.

296 Nepstad, D. C., Stickler, C. M., & Almeida, O. T. (2006). Globalization of the Amazon soy and
297 beef industries: opportunities for conservation. *Conservation biology*, *20*(6), 1595-1603.

298 Parmes, E., Rauste, Y., Molinier, M., Andersson, K., & Seitsonen, L. (2017). Automatic cloud and
299 shadow detection in optical satellite imagery without using thermal bands—Application to Suomi
300 NPP VIIRS images over Fennoscandia. *Remote Sensing*, 9(8), 806.

301 Piao, S., Liu, Q., Chen, A., Janssens, I. A., Fu, Y., Dai, J., ... & Zhu, X. (2019). Plant phenology
302 and global climate change: Current progresses and challenges. *Global Change Biology*, 25(6),
303 1922-1940.

304 Price, K. P., Guo, X., & Stiles, J. M. (2002). Optimal Landsat TM band combinations and
305 vegetation indices for discrimination of six grassland types in eastern Kansas. *International*
306 *Journal of Remote Sensing*, 23(23), 5031-5042.

307 Rudd, D. A., Karami, M., & Fensholt, R. (2021). Towards High-Resolution Land-Cover
308 Classification of Greenland: A Case Study Covering Kobbefjord, Disko and Zackenberg. *Remote*
309 *Sensing*, 13(18), 3559.

310 Sanchez, A. H., Picoli, M. C. A., Camara, G., Andrade, P. R., Chaves, M. E. D., Lechler, S., ... &
311 Queiroz, G. R. (2020). Comparison of Cloud cover detection algorithms on sentinel-2 images of
312 the amazon tropical forest. *Remote Sensing*, 12(8), 1284.

313 Sinergise (2023a). *SentinelHub*. <https://www.sentinel-hub.com/> (accessed on 10 July 2023).

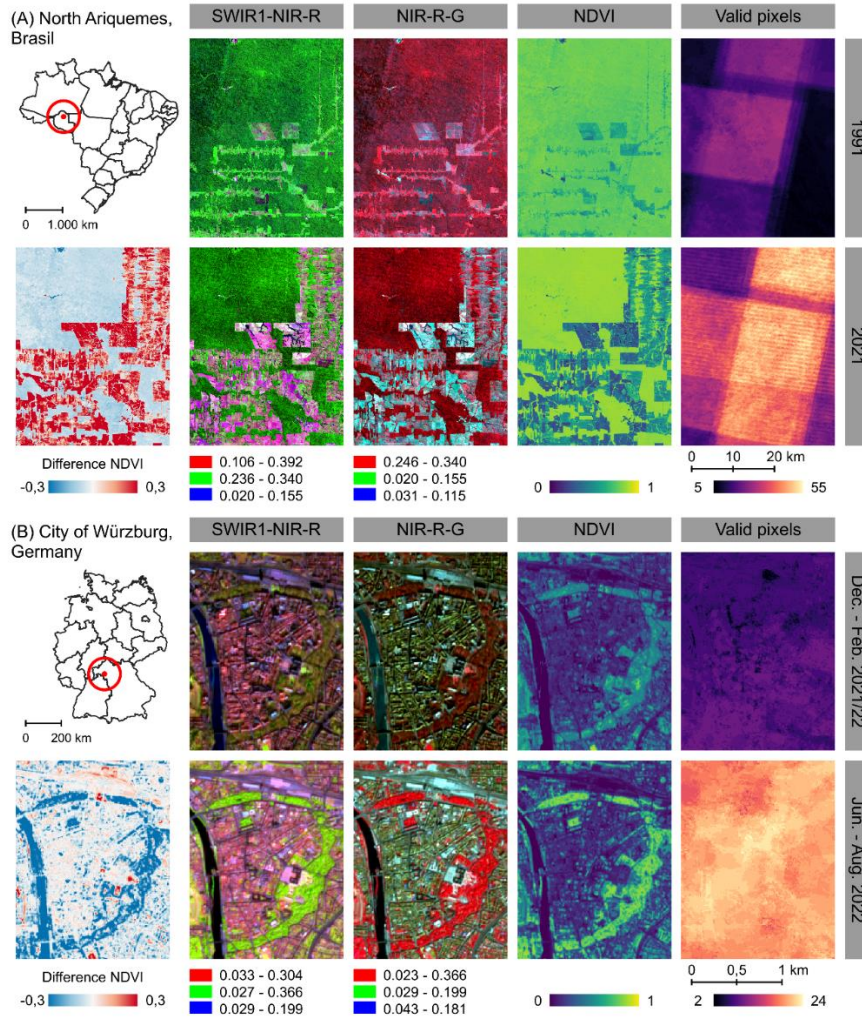
314 United States Geological Survey (2022, August 4). *Landsat - Earth Observation Satellites*. Fact
315 Sheet 2015–3081, ver. 1.4, August 2022. Available at
316 <https://pubs.usgs.gov/fs/2015/3081/fs20153081.pdf>

317 United States Geological Survey (2023). *EarthExplorer*. <https://earthexplorer.usgs.gov/>
318 (accessed on 10 July 2023).

- 319 Verhoeven, V. B., & Dedoussi, I. C. (2022). Annual satellite-based NDVI-derived land cover of
320 Europe for 2001–2019. *Journal of Environmental management*, 302, 113917.
- 321 Weng, Q., Quattrochi, D., Xian, D. (2008). *Special Issue Remote Sensing of Land Surface*
322 *Properties, Patterns and Processes*. MDPI Remote Sensing. Available at
323 [https://www.mdpi.com/journal/sensors/special_issues/remote-sensing-land-surface-](https://www.mdpi.com/journal/sensors/special_issues/remote-sensing-land-surface-properties#published)
324 [properties#published](https://www.mdpi.com/journal/sensors/special_issues/remote-sensing-land-surface-properties#published) (accessed on 11 July 2023).
- 325 Wong, S. T., Guharajan, R., Petrus, A., Jubili, J., Lietz, R., Abrams, J. F., ... & Sollmann, R.
326 (2022). How do terrestrial wildlife communities respond to small- scale Acacia plantations
327 embedded in harvested tropical forest?. *Ecology and Evolution*, 12(9), e9337.
- 328 Yang, W., Chen, X., Wang, C., Cao, R., Zhu, X., Shen, B. (2021). *Special Issue Time Series*
329 *Analysis in Remote Sensing: Algorithm Development and Applications*. MDPI Remote Sensing.
330 [https://www.mdpi.com/journal/remotesensing/special_issues/time_series_algorithm_developme](https://www.mdpi.com/journal/remotesensing/special_issues/time_series_algorithm_development)
331 [nt](https://www.mdpi.com/journal/remotesensing/special_issues/time_series_algorithm_development) (accessed on 11 July 2023).
- 332 Yin, H., Brandão Jr, A., Buchner, J., Helmers, D., Iuliano, B. G., Kimambo, N. E., ... & Radeloff,
333 V. C. (2020). Monitoring cropland abandonment with Landsat time series. *Remote Sensing of*
334 *Environment*, 246, 111873.
- 335 Zeng, Y., Hao, D., Huete, A., Dechant, B., Berry, J., Chen, J. M., ... & Chen, M. (2022). Optical
336 vegetation indices for monitoring terrestrial ecosystems globally. *Nature Reviews Earth &*
337 *Environment*, 3(7), 477-493.
- 338 Zhu, C., Zhang, X., & Huang, Q. (2018). Four decades of estuarine wetland changes in the Yellow
339 River delta based on Landsat observations between 1973 and 2013. *Water*, 10(7), 933.

340 Zhu, Z., Wang, S., & Woodcock, C. E. (2015). Improvement and expansion of the Fmask
341 algorithm: Cloud, cloud shadow, and snow detection for Landsats 4–7, 8, and Sentinel 2 images.
342 *Remote sensing of Environment*, 159, 269-277.

Figures



Options	(A) North Ariquemes (Brasil)	(B) City of Würzburg (Germany)
Satellite platform	Landsat-5,7,8,9	Sentinel-2
Study area	Polygon coordinates (in degree): -63.1 to -62.6 °W, -9.7 to -9.3 °S	Polygon coordinates (in degree): 49.78 to 49.8 °E, 9.92 to 9.94 °N
Month, year, max. cloud cover (per scene)	(1) 1-12, 1991, 65% (2) 1-12, 2021, 65%	(1) 12-2, 2022-23, 65% (winter) (2) 6-8, 2022, 65% (summer)
Number of selected scenes	(1) 44 scenes (2) 97 scenes	(1) 9 scenes (2) 26 scenes
Band selection	B, G, R, NIR, SWIR1, SWIR2, NDVI, valid pixels	
Aggregation mode	median	
Spatial resolution	30 meter	10 meter
CRS	UTM (EPSG: 32620)	UTM (EPSG: 32632)

344 **Figure 1:** Example GEE-PICX products. A: Annual aggregates based on Landsat scenes for 1991 and
 345 2021. B: Seasonal aggregates based on Sentinel-2 scenes for summer (June 2022 - August 2022) and
 346 winter (December 2021 - February 2022). The maps show a subset of the available band information.
 347 The striking pattern in the valid-pixel scenes results from the orbital path overlap of the Landsat satellites
 348 and does not affect image composites. Absolute difference in NDVI was calculated for both areas, with
 349 positive values indicating an increase of NDVI compared to the earlier scene.

350 Supporting Information

351 Supporting Information S1

352 Data processing in GEE-PICX

353 **Table S1:** Functional setup of GEE-PICX application script.

Functionality	Description
Image selection and filtering	Select Landsat / Sentinel-2 surface reflectance (SR) products (Level-2). Filter single scenes by study area, time frame and maximum cloud cover.
Cloud masking *	Landsat SR data: mask clouds, cloud shadows and snow from the Cloud Quality Assessment band (QA_PIXEL bitmask). Sentinel-2 SR data: mask clouds, cloud shadows and highly reflective surfaces with auxiliary S2 cloud probability dataset (s2cloudless).
Band selection	Select and rename S2 bands according to spectral wavelength range Select and rename LS 8 & 9 bands according to spectral wavelength range Select and rename LS 5 & 7 bands according to spectral wavelength range
Scale factor application	Apply scale factor for Landsat SR data (0.0000275 + (- 0.2)) before usage Apply scale factor for Sentinel-2 SR data (0.0001)
Spectral indices calculation	Calculate indices with respective formulas and add as band information to each individual scene

Image aggregation & data quality assessment	Aggregate filtered scenes from year or season by median, mean or standard deviation. Count valid pixels at each pixel location for data quality assessment
Visualization	Aggregated scenes can be added to the map. Users can choose spectral indices as single bands or choose from various 3-band combinations. Further changes can be applied manually in the layer panel box. May fail if data size or area of interest are too large (limitations in Google Earth Engine).
Export preparation	Create a batch task to export images as raster to Google Drive. All image band values are multiplied by 10,000 in advance and converted to signed 16-bit integer to reduce output file size (except for valid-pixel band)

354

355 * Additional information on s2cloudless:

356 The development of the s2cloudless algorithm (Zupanc, 2019) has allowed researchers to refine cloud
 357 masking, resulting in greater confidence in the final analysis. There is currently no equivalent method for
 358 images from the Landsat collection. While the QA60 band is limited to a binary classification of thick and
 359 cirrus clouds (European Space Agency, 2020), s2cloudless generates an image with cloud presence
 360 probabilities ranging from 0 to 100 percent, at 10 meter scale (Braaten et al., 2020). This provides the
 361 opportunity to customize the cloud masking process to better suit the specific requirements of a project.
 362 Higher values of the s2cloudless layer are more likely related to clouds or highly reflective surfaces such
 363 as snow or roof tops (Google Earth Engine, 2023).

364 The s2cloudless layer is a separate data set from which matching scenes are automatically selected and
 365 filtered. The default cloud probability threshold in the application is 50 % to define cloud / non-cloud masks,
 366 which generally allows a very good cloud masking performance (Braaten et al., 2020). The optimal value
 367 for the best performance can depend on factors such as cloud type, cover type, location, etc. Users who

368 wish to further customize the cloud mask need to adjust the variable “isNotCloud” in the application script
369 where cloud masking is applied to the selected Sentinel-2 images. In this case, we suggest experimenting
370 with a few different values to better understand the distribution of cloud probability values. For example,
371 thin clouds may not be detected at 90 % cloud probability threshold, but are detected at 10 % (Braaten et
372 al., 2020). The single scenes from the cloud-masked image collection in the *Console* tab could be used to
373 investigate changes due to cloud mask tuning. Nevertheless, for proper inspection and evaluation, basic
374 knowledge of using the Google Earth Engine API is beneficial. For most use cases it is not necessary to
375 modify the cloud probability threshold.

376

377 **References**

378 Braaten, J., Schwehr, K., Ilyushchenko, S. (2020). *More accurate and flexible cloud masking for*
379 *Sentinel-2 images*. Available online: [https://medium.com/google-earth/more-accurate-and-](https://medium.com/google-earth/more-accurate-and-flexible-cloud-masking-for-sentinel-2-images-766897a9ba5f)
380 [flexible-cloud-masking-for-sentinel-2-images-766897a9ba5f](https://medium.com/google-earth/more-accurate-and-flexible-cloud-masking-for-sentinel-2-images-766897a9ba5f) (accessed on 11 July 2023).

381 European Space Agency (2022). *Sentinel-2*. ESA. Sentinel-2 User Handbook; ESA: Paris,
382 France, 2015; p. 64. Available at: [https://sentinel.esa.int/documents/247904/685211/Sentinel-](https://sentinel.esa.int/documents/247904/685211/Sentinel-2_User_Handbook)
383 [2_User_Handbook](https://sentinel.esa.int/documents/247904/685211/Sentinel-2_User_Handbook).

384 Google Earth Engine (2023). *Sentinel-2: Cloud Probability*. Available online:
385 [https://developers.google.com/earth-](https://developers.google.com/earth-engine/datasets/catalog/COPERNICUS_S2_CLOUD_PROBABILITY#description)
386 [engine/datasets/catalog/COPERNICUS_S2_CLOUD_PROBABILITY#description](https://developers.google.com/earth-engine/datasets/catalog/COPERNICUS_S2_CLOUD_PROBABILITY#description) (accessed 11
387 July 2023).

388 Zupanc, A (2019). Improving Cloud Detection with Machine Learning. Available online:
389 [https://medium.com/sentinel-hub/improving-cloud-detection-with-machine-learning-](https://medium.com/sentinel-hub/improving-cloud-detection-with-machine-learning-c09dc5d7cf13)
390 [c09dc5d7cf13](https://medium.com/sentinel-hub/improving-cloud-detection-with-machine-learning-c09dc5d7cf13) (accessed on 11 July 2023).

391 Supporting Information S2

392 Satellite data available in GEE-PICX.

393

394 **Table S2:** Information on satellite data accessible from GEE-PICX web application.

Platform	Sentinel-2		Landsat			
Mission	Sentinel-2A	Sentinel-2B	Landsat-5	Landsat-7	Landsat-8	Landsat 9
Mission	2015-06-23	2017-03-07	1984-03-01	1999-04-15	2013-02-11	2021-09-27
Launch						
Data availability in GEE-PICX app	2017-03-28 - present		1984-03-16 - 2012-05-05	1999-05-28 - present	2013-03-18 - present	2021-10-31 - present
Sensor*	MSI		MSS + TM	ETM+	OLI + TIRS	OLI + TIRS
Temporal resolution	10-days each, 5-days combined constellation		16-days each, 8-days combined constellation Landsat-8 and 9			
Spatial resolution	10-meter		30-meter			
Spectral resolution**	<i>Bands 2-5, 8, 8A, 11-12:</i> visible, NIR, red-edge, SWIR		<i>Bands 1-5, 7:</i> visible, NIR, SWIR		<i>Bands 2-7:</i>	
Spectral & spatial resolution (bands, in meter)	<i>Bands 2-5, 8, 8A, 11-12:</i> 10 m: R, G, B, NIR; 20 m: Red-edge, SWIR		<i>Bands 1-5, 7:</i> 30 m: B, G, R, NIR, SWIR	<i>Bands 1-5, 7:</i> 30 m: B, G, R, NIR, SWIR	<i>Bands 2-7:</i> 30 m: B, G, R, NIR, SWIR	<i>Bands 2-7:</i> 30 m: B, G, R, NIR, SWIR

**Additional
information**

- - - Scan Line - -
Corrector
(SLC) failure
since 2003-
05-31
(22 percent of
each image
affected by
data gaps)

Operator***

ESA

NASA & USGS

-
- 395 * OLI, Operational Land Imager; TIRS, Thermal Infrared Sensor; ETM+, Enhanced Thematic Mapper Plus; TM, Thematic Mapper;
 - 396 MSS, Multispectral Scanner; MSI, Multispectral Instrument
 - 397 ** Visible: blue, green, red; NIR: near-infrared; SWIR: shortwave-infrared
 - 398 *** ESA, European Space Agency; NASA, National Aeronautics and Space Administration; USGS, United States Geological Survey

399 Supporting Information S3

400 Spectral Indices available in GEE-PICX

401

402 **Table S3:** Available spectral indices derived from Landsat or Sentinel-2 imagery.

Band name	Full name	Formula	Interpretation
NDVI	Normalized Difference Vegetation Index	$\frac{(NIR - Red)}{(NIR + Red)}$	Highlights density and health of photosynthetically active vegetation. Tends to saturate in densely vegetated areas. Sensitive to the contribution of soil brightness and atmospheric effects..
EVI2	Enhanced Vegetation Index 2	$2,4 * \frac{(NIR - Red)}{(NIR + Red + 1)}$	Highlights photosynthetically active vegetation, but does not saturate in densely vegetated areas. Accounts for soil brightness variation. Less affected by atmospheric effects than NDVI and EVI.
SAVI	Soil-Adjusted Vegetation Index	$\frac{(NIR - Red)}{(NIR + Red + L)} * (1 + L)$	Highlights photosynthetically active vegetation and accounts for soil brightness variation.
MSAVI	Modified Soil-Adjusted Vegetation Index	$\frac{(NIR - Red)}{(NIR + Red + L_0)} * (1 + L_0)$	Modified version of SAVI to further minimize the soil background influences on the vegetation signal.

NDMI	Normalized Difference Moisture Index	$\frac{(NIR - SWIR1)}{(NIR + SWIR1)}$	Sensitive to moisture levels in vegetation and soil. Useful for vegetation analyses, for identifying areas prone to drought stress or excess moisture.
NBR	Normalized Burn Ratio	$\frac{(NIR - SWIR2)}{(NIR + SWIR2)}$	Detects and quantifies burnt areas. In general, low NBR values indicate recently burnt areas and bare ground.
NBR2	Normalized Burn Ratio 2	$\frac{(SWIR1 - SWIR2)}{(SWIR1 + SWIR2)}$	A modification of the NBR, useful in postfire recovery studies, highlights vegetation with high water content.
BSI	Bare Soil Index	$\frac{(SWIR1 + Red) - (NIR + Blue)}{(SWIR1 + Red) + (NIR + Blue)}$	Highlights bare ground and rock surfaces. Useful in identification of soil erosion, land degradation, and urbanization processes.
NDWI	Normalized Difference Water Index	$\frac{(Green - NIR)}{(Green + NIR)}$	Sensitive to water bodies. Useful for water resource management, wetland monitoring, and flood assessment.

403

404 For more information on spectral indices see: Petropoulos & Kalaitzidis (2012), Zeng et al.
405 (2022), United States Geological Survey (2022), Qi et al. (1994), Keeley (2009).

406 **References**

407 Keeley, J. E. (2009). Fire intensity, fire severity and burn severity: a brief review and suggested
408 usage. *International journal of wildland fire*, 18(1), 116-126.

409 Petropoulos, G. P., & Kalaitzidis, C. (2012). Multispectral vegetation indices in remote sensing:
410 an overview. *Ecological Modeling*, 2, 15-39.

411 Qi, J., Chehbouni, A., Huete, A. R., Kerr, Y. H., & Sorooshian, S. (1994). A modified soil adjusted
412 vegetation index. *Remote sensing of environment*, 48(2), 119-126.

413 United States Geological Survey (2022, August 4). *Landsat - Earth Observation Satellites*. Fact
414 Sheet 2015–3081, ver. 1.4, August 2022. Available at
415 <https://pubs.usgs.gov/fs/2015/3081/fs20153081.pdf>

416 Zeng, Y., Hao, D., Huete, A., Dechant, B., Berry, J., Chen, J. M., ... & Chen, M. (2022). Optical
417 vegetation indices for monitoring terrestrial ecosystems globally. *Nature Reviews Earth &*
418 *Environment*, 3(7), 477-49